JOURNAL OF GEOPHYSICAL RESEARCH, VOL. 111, C06015, doi:10.1029/2004JC002357, 2006

Formation and pathways of intermediate water in the Parallel Ocean Circulation Model's Southern Ocean

Mathijs W. Schouten[1,2] and Ricardo P. Matano[1]

Received 1 March 2004; revised 30 December 2005; accepted 13 February 2006; published 13 June 2006.

[1] The formation mechanisms and pathways of intermediate water in the Southern Ocean are analyzed from output of a high-resolution ocean general circulation model. Deep winter mixed layer formation in the Southern Ocean is diagnosed from the model results and is found to be mostly consistent with observations. Diapycnal water mass transformations by air-sea fluxes and internal mixing are quantified and split into mean and eddy components. The diapycnal formation of the water masses that constitute the Antarctic intermediate water layer in the southeast Pacific is found to occur mainly in the western Pacific Ocean in this model. In winter, convection up to 900 m is found to set the potential vorticity characteristics of this layer. Eddy fluxes of heat and buoyancy play an important role in the formation of the intermediate waters by transferring water from the southern parts of the subtropical gyres into the Antarctic Circumpolar Current (ACC) and vice versa. The effects of eddy fluxes are found to vary significantly along the path of the ACC. They are strongly concentrated in the regions near the Agulhas Return Current in the Indian Ocean and the Brazil-Malvinas Confluence in the Atlantic.

Citation: Schouten, M. W., and R. P. Matano (2006), Formation and pathways of intermediate water in the Parallel Ocean Circulation Model's Southern Ocean, *J. Geophys. Res.*, *111*, C06015, doi:10.1029/2004JC002357.

1. Introduction and Background

[2] In recent years, the importance of the Southern Ocean and the Antarctic Circumpolar Current (ACC) in the global ocean circulation has become clear. Both from observational and modeling viewpoints, the role of the ACC in the transformation of water masses, the exchange of water between adjacent ocean basins, and the associated links in the global thermohaline circulation have been stressed [*Döös*, 1994; *Speer et al.*, 2000; *Sloyan and Rintoul*, 2001b; *Webb and Suginohara*, 2001; *Talley*, 2003]. The formation of cold and fresh intermediate waters near the northern boundary of the ACC is one of the central issues in the study of the Southern Ocean's impact on the global circulation and climate. The formation, pathways and modification of intermediate waters through the Southern Ocean form an important, though poorly sampled link in our understanding of the world oceans [*Sloyan and Rintoul*, 2001a; *Talley*, 2003]. The crucial role played by the intermediate waters of the Southern Ocean in the transformation of cold North Atlantic deep water into warmer thermocline waters justifies a thorough investigation of the pathways and formation mechanisms of these waters. Also, these intermediate waters may act as a buffer for climate change. As one of the primary ventilation mechanisms of the ocean, the intermediate waters of the Southern Ocean may for some time moderate changes in the concentrations of gases such as CO_2 in the atmosphere. The increased temperatures in the Antarctic intermediate water levels observed by *Gille* [2003] seem to indicate another way by which the Southern Ocean may act as a buffer for climate change, by absorbing heat into the ocean. The importance of the Southern Ocean in absorbing heat under present-day and changing climate conditions has been clearly demonstrated in a coupled ocean-atmosphere model [*Gregory*, 2000].

[3] Several mechanisms for the formation of Antarctic intermediate water have been proposed. The early concept of continuous formation all around the ACC [*Wüst*, 1935], has long been replaced by recognition of the importance of the waters east and west of Drake Passage [*McCartney*, 1977; *Gordon et al.*, 1977; *Molinelli*, 1981], although the latter also suggest the Kerguelen region in the Indian Ocean sector of the ACC as a region of active injection of Antarctic intermediate water (AAIW). The winter mixed layers of the southeast Pacific are the deepest and coldest of their kind, and the densest Subantarctic mode water (SAMW) of the eastern Pacific has been recognized as the precursor of AAIW [*McCartney*, 1977; *Molinelli*, 1981]. However, the freshest AAIW in the Atlantic is colder than the SAMW in the Pacific, which led *Piola and Georgi* [1982] to conclude that a source of AAIW had to be present near the polar front in the South Atlantic. This was supported by hydrographic observations in the Drake Passage and Malvinas Current region [*Piola and Gordon*, 1989]. Winter cooling and

[1] College of Oceanic and Atmospheric Research, Oregon State University, Corvallis, Oregon, USA.
[2] Department of Physical Oceanography, Royal Netherlands Institute for Sea Research, Texel, Netherlands.

0148-0227/06/2004JC002357$09.00

cross-frontal mixing in the western Atlantic thus cannot be neglected. Eddy flux convergence north of the Polar front has been suggested as an additional mechanism of AAIW formation [*Karsten et al.*, 2002].

[4] In this paper, we analyze the formation of mode waters and the diapycnal fluxes that lead to the formation of the intermediate waters in the Southern Ocean of an eddy-permitting global ocean general circulation model. We focus on the role of these waters in the interocean exchanges and global meridional overturning circulation. Also, we describe some of the mechanisms responsible for the water mass transformations in the model. We estimate the role of air-sea interaction, eddy fluxes across the ACC and assess their role in the global water mass budgets. The aim of this study is not to assess the degree of realism achieved by the model. The model has been thoroughly validated against observations, and its behavior is relatively well known [e.g., *Stammer et al.*, 1996; *Tokmakian and Challenor*, 1999]. The model was spun up for 30 years and run in diagnostic mode for another 20 years. We use results that correspond to the period 1979–1998.

[5] Our goal is rather to advance our understanding of the dynamic/thermodynamic process that control the model circulation. Previous investigations, such as those by *England* [1993] have shown how model parameterizations are of prime importance for the correct representation in low-resolution models of crucial water masses such as the intermediate waters of the Southern Ocean. The formation of AAIW near Drake Passage in the Pacific and Atlantic oceans by convection was reproduced by a coarse-resolution numerical model simulation [*England et al.*, 1993]. In a similar model, but with different surface forcing [*Sorensen et al.*, 2001] investigated the sensitivity of AAIW formation to different mixing schemes, and concluded that isopycnal mixing and subduction along the SAF dominate the AAIW formation in a coarse resolution model including the *Gent and McWilliams* [1990] parameterization for eddy-induced transport. Midlatitude and subpolar convection are reduced by the stronger stratification allowed for by this parameterization [*Santoso and England*, 2004, and references therein].

[6] The numerical simulation used here was performed by R. Tokmakian using the Parallel Ocean Circulation Model (POCM) [*Tokmakian and Challenor*, 1999]. We use results from the experiment POCM-4C that was run for the 19-year period 1979–1998. The model is defined on a Mercator grid with an average grid size of 0.25°. The bottom topography of the model was derived from the 1/12° ETOPO5 data set. From 1979 to 1994 the model was forced with daily atmospheric fluxes derived from the European Center for Medium-range Weather Forecast (ECMWF) reanalysis; after that time period the forcing fluxes were replaced with operational ECMWF data sets. There is no separate treatment of mixed layer physics. South of 68°S, the upper 2000 m of the model are restored toward climatology using a restoring period of 90 days, to reflect water mass transformations south of the model domain (which ends at 75°S) and resulting from interaction with the sea ice around Antarctica, which is not modelled explicitly. The model does not incorporate an active mixed layer model and diffusion is horizontal rather than along isopycnals. These model limitations may play a role in the analysis of deep winter mixed layer formation and diapycnal water mass transformations. For the purposes of this article, we use 3-day averages (separated by 9 days) of model outputs of temperature, salinity, and velocity corresponding to the period 1986–1998. A more detailed description of the model equations and numerical algorithms can be found in the work by *Stammer et al.* [1996, and references therein].

[7] Since the issue of the equilibrium of these types of model leads to confusion it is convenient to clarify what is the rationale that was used to design the integration strategy. The oceanic adjustment has three basic timescales: the longer is the diffusive, which is associated with the formation of the thermocline. This is the timescale of climate studies models that are started from scratch and forced with surface fluxes. These type of models need to be integrated for thousands of years before reaching dynamical and thermodynamical equilibrium. The second timescale is associated with the adjustment of the oceanic circulation to wind forcing. Models used in these types of studies have a thermocline but that are otherwise at rest (i.e., the thermocline is flat). The adjustment of these models is accomplished by the propagation of planetary waves and the consequent building of the thermocline slope and is of the order of decades (at midlatitudes). The third timescale corresponds to the type of modeling that we are analyzing, and are those that are initialized with observations. In this case the model already has a thermocline and that thermocline has a slope. The adjustment therefore is more rapid and is mostly associated with the advective adjustment of geostrophic currents (of the order of months). It should be noted that the last two types of models reach dynamical equilibrium but not thermodynamical equilibrium; that is, very long integrations of these types of model suffer the so-called climate drift. That is, their density structure departs significantly from the initial conditions because of incompatibilities among the initial and boundary conditions and internal model parameterizations (e.g., vertical or horizontal mixing). If the integrations are long enough to reach advective (and wave) adjustment but short enough to avoid climate drift then the model produces a density field that is in dynamically consistent with the wind and the bottom topography (something which the highly smoothed and interpolated hydrographic data is not) and it also produces the entire field of velocities (including the vertical ones). This type of studies therefore use numerical models to combine information of hydrography, with bottom topography and surface fluxes to obtain a comprehensive view of the ocean circulation.

[8] Following this line of thought, we present an analysis of diapycnal fluxes inferred from the divergence of the horizontal velocities in isopycnal layers. Divergence of isopycnal flow can only be interpreted as diapycnal formation under the assumption of steady state. In POCM there is a small drift due to the parameterization of vertical mixing but since the length of the numerical integration is smaller than the diffusive timescale $T_{\mathrm{dif}} \sim H^2/K_v \sim$ 120 years, where H is a scale depth ($\sim$2000 m), and K_v a typical value of the vertical eddy diffusivity used in the model ($\sim 10^{-3}$ m^{2}s^{-1}) the water mass structure of the model is still very close to the observations and

the changes in its distribution can be attributed to dynamic effects.

2. General Analysis

2.1. Description of the Circulation

[9] Before going into details of the diapycnal fluxes in the Southern Ocean of the POCM, we give a general description of the simulated ACC, its variability and connections to the subtropical basins.

[10] The total mean transport of the ACC through Drake Passage is 163 Sv. *Gille* [1997] shows for an older version of the POCM model that topographic form stresses are largely acting in three regions: the Kerguelen Plateau in the Indian Ocean, the Campbell Plateau south of New Zealand, and the Drake Passage connecting the Atlantic and Pacific oceans (see Figure 1). The distributions of eddy kinetic energy simulated by the POCM (which is strongly concentrated in these three regions), and estimates of eddy kinetic energy obtained from satellite altimetry (showing maxima near several more bottom topographic features) suggest that the POCM may not fully capture the interactions between the flow and the smaller topographic features of the Southern Ocean. The resulting underestimation of ACC bottom topography interaction may be the cause of the somewhat higher transport in the POCM model compared to observations.

[11] The stream function of the mean vertically integrated flow in the POCM (Figure 1) shows a concentration of the flow near these three topographic obstructions, but also the other major topographic features in all three oceans can be recognized in the stream function distribution. Clockwise circulation in the Weddell and Ross seas is observed, although the absence of an ice model reduces confidence in the realistic nature of particular details in those regions. The vertically integrated stream function also shows the major features of the subtropical gyre circulation in the southern hemisphere. The strongest of the three subtropical western boundary currents is that of the South Indian Ocean, where the model reproduces the strong recirculation in the southwestern part of the basin [*Stramma and Lutjeharms*, 1997] and the mean circulation resulting from the frequent passage of Agulhas rings [*Byrne et al.*, 1995; *Schouten et al.*, 2000]. The model produces only 2–3 rings per year, but the mean and eddy fluxes of mass, heat and salt associated with them are very similar to those estimated from observations and higher resolution models, where 5–8 Agulhas rings per year are found [*Matano and Beier*, 2003; *De Ruijter et al.*, 1999]. The subtropical gyre of the Atlantic is connected to that of the Indian via the so-called supergyre [*De Ruijter*, 1982]. About 20 Sv circulates through this large conceptual gyre, reaching as far east as the eastern tip of the Australian continent (Figure 1). The western boundary current of the Atlantic, the Brazil Current, meets the ACC at the Brazil-Malvinas confluence. This confluence region in the South Atlantic, and the Agulhas Retroflection region in the South Indian Ocean are the two places where the ACC and subtropical warmer waters are in closest vicinity to each other, and, as both are also regions of high eddy variability, where ACC-subtropical interactions are most likely to occur. In this paper we show that this is the case in the POCM simulation. In the Pacific Ocean, no such region of strong gyre-ACC interaction is found, mostly due to the fact that the East Australian Current is much weaker than the Agulhas and Malvinas Currents [*Chiswell et al.*, 1997], and the loss of upper and thermocline waters to the Indian Ocean via the Indonesian Throughflow [*Wijffels et al.*, 1992; *Ganachaud et al.*, 2000]. Pacific-Indian Ocean exchange of intermediate water via "Tasman Leakage" south of Australia is yet another contribution to the warm water limb of the global meridional overturning circulation [*Speich et al.*, 2001; *Sloyan and Rintoul*, 2001b].

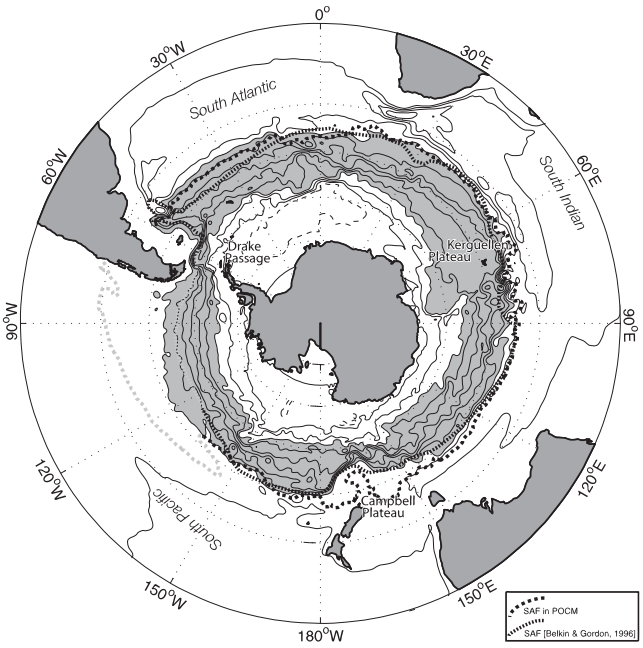

Figure 1. Mean vertically integrated stream function. Contours are drawn 20 Sv apart, and the region between 40 and 160 Sv is shaded. This region encompasses most of the ACC and is the focus of several of our analyses. Two estimates of the location of the Subantarctic front have been overlaid (dashed lines): the front based on the mean salinity field of POCM using the definition of *Patterson and Whitworth* [1990] and the front as determined by *Belkin and Gordon* [1996], which is based on evaluation of a large collection of in situ conductivity-temperature-depth observations. In the southeast Pacific, both estimates are poorly defined, and both are denoted by gray lines.

[12] The most relevant front of the ACC in the context of AAIW formation is the Subantarctic front, which can be considered the boundary between the Antarctic Circumpolar Current and the subtropical circulation. A wide range of identifying characteristics has been proposed (for a summary, see *Belkin and Gordon* [1996]). Here we apply the definition used by *Whitworth and Nowlin* [1987] and *Patterson and Whitworth* [1990], who identified the SAF in the long-term mean salinity field by a rapid descent of the subsurface salinity minimum from around 200 m to around 1000 m depth. The thus defined SAF in the model (thick dashed line in Figure 1) follows both the 160 Sv streamline and the observed SAF given by *Belkin and Gordon* [1996] (thin dashed line) along most of its trajectory. The most notable difference between the observed SAF location and

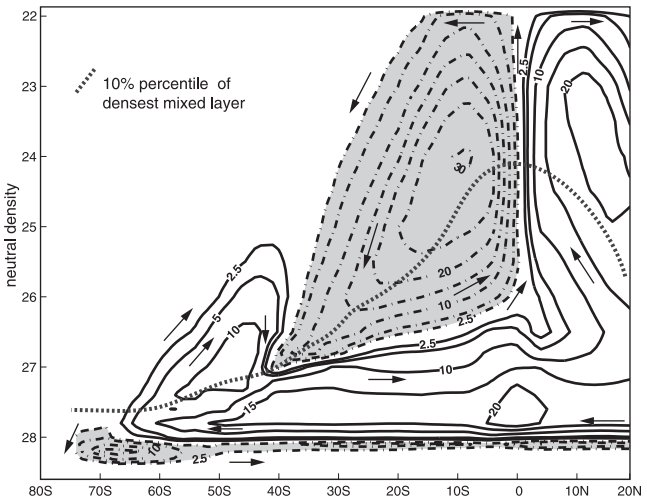

Figure 2. Zonally integrated meridional overturning in neutral density coordinates. To indicate the position of the mixed layer, we evaluated the maximum surface layer density in the monthly mean fields. The dotted line shows the 10% percentile along latitude circles and can be considered a lower bound of the maximum mixed layer density at each latitude.

that from the POCM is in the southeast Pacific, where both are poorly defined as the salinity minimum is not well defined [*Belkin and Gordon*, 1996; *Chaigneau and Pizarro*, 2005]. Other differences are found on both sides of the Campbell plateau and in Drake Passage. Especially the deviations near the Campbell Plateau may be important, as we find this region to be particularly important in the formation of AAIW (see section 2.3).

[13] In the Southern Ocean, the mean meridional circulation is better represented in density coordinate than in the zonally integrated z level stream function [*Döös and Webb*, 1994; *Gregory*, 2000]. In Figure 2 we show the zonally integrated meridional overturning stream function in neutral density coordinates for the region south of 20°N. The meridional overturning in density coordinates is, in the upper layers (γ_n < 26.0), dominated by the combined transports of the subtropical gyres. Their combination leads to a 30 Sv cell with lighter (γ_n < 25.0) waters flowing away from the equator, mainly in the western boundary currents of the Indian and Atlantic oceans, and a return flow (25.0 < γ_n < 26.0) of intermediate density thermocline waters in the interior of the gyres between the equator and 40°S. The global meridional overturning simulated by the POCM model in z coordinates can be found, for example, in work by *Jayne and Marotzke* [2001]. *Gregory* [2000] shows how upward diffusion and downward advection of heat balance in a coupled ocean-atmosphere model. Along-isopycnal diffusion of heat is the dominant term as the density structure is determined by salinity in the cold upper layers of the Southern Ocean. The dashed line in Figure 2 shows which part of the overturning occurs within the mixed layer. It denotes the densest mixed layer density occurring seasonally at each latitude, so is a lower bound of the mixed layer position. The 10 Sv clockwise cell in the Southern Ocean is found to be mostly confined to the mixed layer, and is associated with the seasonal warming and cooling of the mixed layer.

[14] The circulation in the deeper levels is dominated by the meridional overturning of North Atlantic Deepwater (NADW, $\gamma_n \approx 28.0$) which is characterized by southward flow of 16 Sv flowing south from the North Atlantic to 55°S, and return flow in the intermediate density classes. The northward flow of Antarctic bottom water (AABW) into the Atlantic and Indian oceans is prohibited by the model bottom topography, resulting in a relatively weak (<3 Sv) meridional cell below the NADW cell and a relatively strong but local cell south of 60°S. The narrow channels through which the deep basins are connected are poorly resolved by the 0.4° bottom topography used in the POCM. For example, the Vema Channel, which carries most of the AABW into the Atlantic, is closed below 3000 m.

[15] Between the subtropical cell and the NADW there is northward transport of intermediate water (26.8 < γ_n < 27.5). In order to investigate the formation and pathways of the intermediate waters in the Southern Ocean of the POCM, we follow a twofold approach. First, we investigate the occurrence and nature of the mode water formation in the model. We provide an inventory of deep mixed layer occurrence in the model, and compare their characteristics to available observational information (section 2.2). Second, we analyze the diapycnal fluxes in the 12 year model run, and identify the main regions of diapycnal formation, the pathways, and transformation regions for the intermediate waters of the Southern Ocean (section 2.3).

2.2. Mode Water Formation

[16] The off-line analysis of 3-day averaged fields from the model does not allow us to directly diagnose the convective events that set the final characteristics of the mode waters of the Southern Ocean. We can, however, diagnose the results of convection, by identifying the marginally stable layers that reach from the surface to a certain depth into the ocean. These marginally stable layers are good indicators of where convection occurs, how deep it reaches, and which density classes are involved. The stable layers usually exist until the next summer provides the heating necessary for restratification.

[17] We define a marginally stable layer as a layer for which $\sigma_0(z) < \sigma_0$ (surface) +0.01 kg/m^3. Deep mixed layers are those layers which are marginally stable to at least 100 m depth, and occur in winter. The total area of such layers in the southern hemisphere shows a very regular annual cycle, which peaks in August after a rapid buildup during winter. As the main water mass characteristics are set during winter when the mixed layer is deepest, we show the mean August mixed layer depths and densities (Figures 3 and 4). In Figures 3 and 4, the Subantarctic front has been included, which illustrates the crucial role of the southeast Pacific ocean in the formation of AAIW.

[18] The depths of the mixed layers simulated by the model (Figure 3) are large compared to values indicated by observations [*Hanawa and Talley*, 2001, Plate 5.4.2]. Direct observations of winter mixed layer depths are very sparse, and the results of *Hanawa and Talley* [2001] are based on indirect observations. The 95% oxygen saturation level is used as a proxy for wintertime ventilation. The general

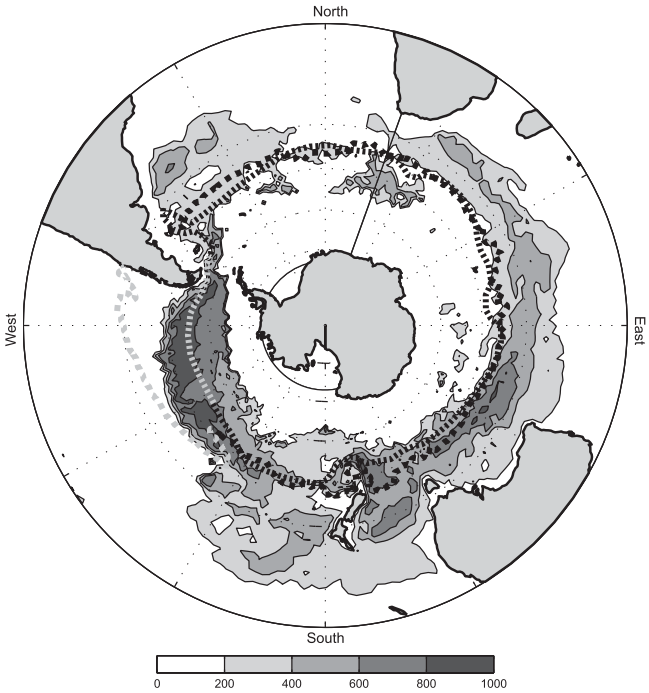

Figure 3. Mean model mixed layer depth during August. The Subantarctic fronts determined both from the model (thick dashed line) and hydrography [*Belkin and Gordon*, 1996] (thin dashed line) have been overlaid. In the southeast Pacific, both are not well determined and are shaded gray here.

pattern and geographic distribution are in agreement with observations. In the western Atlantic and Pacific subtropical gyres surface mixed layers of over 600 m are diagnosed, which is deep compared to observations [e.g., *Hanawa and Talley*, 2001], although the locations of subtropical mode water formation in the recirculations near the western boundaries are realistically represented. Over the Atlantic sector of the Southern Ocean, surface mixed layer depths are patchy and generally small. Over the South Indian Ocean mixed layer depths are consistently deepening toward the east. *Hanawa and Talley* [2001] attribute this deepening to the strong diapycnal fluxes caused by the atmosphere-ocean fluxes in this part of the ocean [*Speer et al.*, 2000].

[19] A large region of rather deep surface mixed layers is found south of Australia, extending as far east as New Zealand, the formation region of the Southeast Indian Subantarctic mode water [*McCarthy and Talley*, 1999]. Further east, along the northern edge of the ACC in the Pacific, the deepest winter mixed layers (up to 900 m) are found. *Tsuchiya and Talley* [1996] reported convection up to 600 m on the basis of oxygen levels. The global pattern of convection depth which indicates rather deep convection in the southeast Indian Ocean north of the SAF and the deepest convection of the southern hemisphere in the southeast Pacific, south of the SAF, is in good agreement with observations.

[20] The mode waters in the subtropical regions of the POCM have potential densities $\sigma_0 \approx 26.0–26.5$ (Figure 4), which compares well with the observed values of $\sigma_0 \approx 26.0$ for the South Pacific, and $26.2 < \sigma_0 < 26.6$ for the South Atlantic [*Hanawa and Talley*, 2001]. The large region of mode water formation south of the Indian Ocean subtropical gyre, and south of Australia, has deep winter mixed layers with median densities between $\sigma_0 = 26.5$ and $\sigma_0 = 27.0$. *Hanawa and Talley* [2001] use 26.8 to characterize the Southeast Indian Subtropical mode water, and 27.0 is the densest SAMW found in the Indian Ocean by *McCartney* [1982], both of which are reproduced in the model results. In the South Pacific the model densities agree reasonably well with observations, although there the model has mixed layers that are slightly denser than those observed: along the southern boundary of the gyre the deep winter mixed layers have densities $27.0 < \sigma_0 < 27.25$. In the southeast Pacific, mode waters of $27.25 < \sigma_0 < 27.5$ are found in the model. *Hanawa and Talley* [2001] use the $\sigma_0 = 27.1$ level to characterize the AAIW of the South Pacific, although often values as high as 27.4 are used [*Sloyan and Rintoul*, 2001a].

2.3. Isopycnal Analysis

[21] As a first step in defining the processes that participate in the water mass transformations, we computed the volume transports in neutral density layers. The mean convergence or divergence of water within a density layer is equivalent to the removal or formation of water due to diapycnal processes, under the assumption of steady state. The model drift over the 10 year period 1986–1996 was found to be small. Over this period, density changes in the upper 1000 m are below 0.1 kg/m^3 for most of the Southern hemisphere, and below 0.3 kg/m^3. As diapycnal transfor-

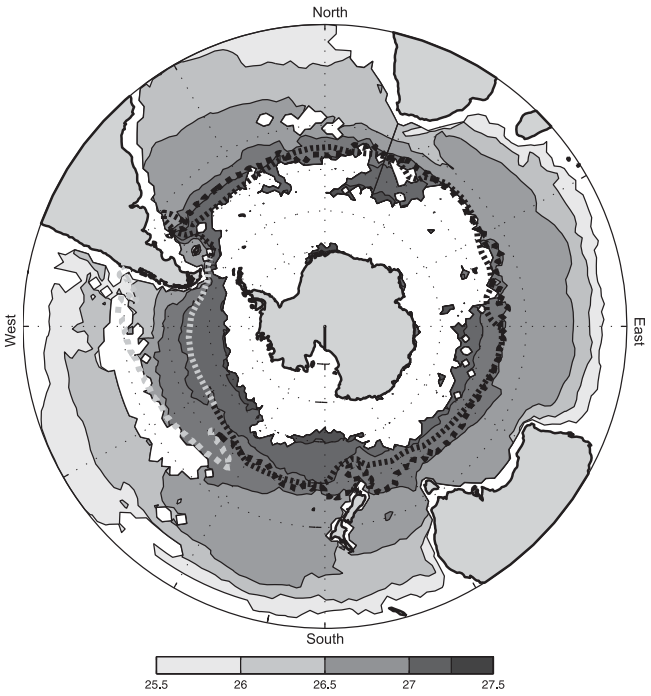

Figure 4. Mean model mixed layer density (σ_0) during August. The Subantarctic fronts determined both from the model (thick dashed line) and hydrography [*Belkin and Gordon*, 1996] (thin dashed line) have been overlaid. In the southeast Pacific, both are not well determined and are shaded gray here.

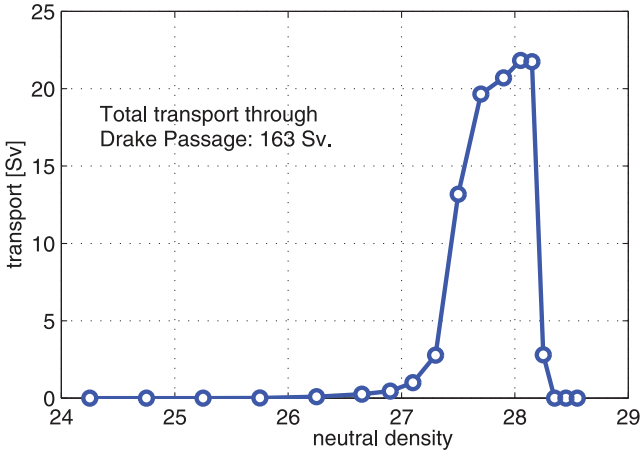

Figure 5. Mean model transport of the ACC in density classes. Units are in Sv per 0.1 neutral density interval. The bulk of the 163 Sv is contained in the $27.4 < \gamma_n < 28.2$ density range.

mations are found to modify water masses at far higher rates, we neglected possible model drift. We computed the isopycnal transports in 4° × 4° boxes between 70°S and 20°N.

[22] The mean flow of the ACC through Drake Passage into the Atlantic (Figure 5) shows very little seasonal variation in the isopycnal transport. Of the total Drake Passage transport, only 2 Sv is in density classes lighter than 27.0, and 8 Sv is in the range $27.0 < \gamma_n < 27.4$. Most of the transport through Drake Passage is in the denser classes: 66 Sv in the range $27.4 < \gamma_n < 27.8$ and 88 Sv denser than $\gamma_n = 27.8$. The "normal" AAIW density range $27.0 < \gamma_n < 27.4$ thus carries substantially less intermediate water through Drake Passage than the 28 Sv estimated from hydrographic inversion by *Sloyan and Rintoul* [2001a]. The POCM seems to have its Antarctic intermediate water (AAIW) at somewhat denser levels than indicated by the observations. To define AAIW in the context of this model, we took a salinity section through a late winter snapshot of the model, and overlaid this section by its neutral density contours (Figure 6).

[23] The results of convection are clearly visible in the vertical isopycnals between 50°S and 60°S. Here, winter cooling has cooled the upper layers enough to overcome the stabilizing effect of decreasing salinity toward the surface. The low-salinity tongue, characteristic of the Antarctic intermediate water, is clearly present north of 55°S, and extends all the way north to the equator at depths of around 1000 m. Figure 6 shows that the density range exposed to deepest convection in the southeast Pacific is $27.4 < \gamma_n < 27.8$. The Antarctic intermediate water in the model can thus be defined as the density layer with $27.0 < \gamma_n < 27.8$, the lighter half ($\gamma_n < 27.4$) of which is not transported through Drake Passage, but stays in the Pacific gyre. The denser half of the AAIW range ($27.4 < \gamma_n < 27.8$) is the model's equivalent of the original AAIW that is transported all around the southern hemisphere.

2.3.1. Transports in Isopycnal Layers

[24] In Figure 7, we show the total zonal transport in the region south of 30°S (solid line), and the meridional transport through 30°S accumulated per basin from the west (dashed line). Positive values denote eastward and northward flow respectively. The total transport (top plot) is split up in four density classes (bottom plots). The solid line can be interpreted as the combined eastward transport of the ACC with contributions from the subtropical gyres. The latter, depicted by the dashed lines, shows generally southward flow near the western boundaries, which is recirculated to the north over the rest of the basin.

[25] The total transport (Figure 7a) shows the 163 Sv total ACC transport through Drake Passage south of South America and south of Africa. South of Australia, this value is augmented by a 10 Sv of water that circulates around Australia through the Indonesian passages, adding up to 173 Sv. On top of that, the subtropical gyres of the Indian, Pacific and Atlantic oceans add about 35, 25 and 25 Sv respectively. The Indian Ocean gyre transport seems low as observations suggest a western boundary current transport of 70 Sv in the Agulhas Current [*Beal and Bryden*, 1999] although *Talley* [2003] reports a closed circulation of 40.5 Sv in the South Indian subtropical gyre, close to our estimate. Much of the larger transport is in a tight recirculation cell that is present in the POCM model too, but somewhat further south. *Matano and Beier* [2003] report an increase from 43 to 68 Sv between 32°S and the tip of the continent on the basis of the same model simulation we study here. The Pacific and Atlantic gyre transports are in reasonable agreement with hydrographic estimates of 18 Sv [*Peterson and Stramma*, 1991] for the Brazil Current and 22–42 Sv [*Chiswell et al.*, 1997] for the East Australian Current.

[26] The dashed lines in Figure 7a show the contribution to the flow south of 30°S made by the three gyres. We accumulated the northward flow through 30°S separately within each of the ocean basins, which highlights the transport in the western boundary layers, and the broad northward compensating flow in the rest of the basins. The

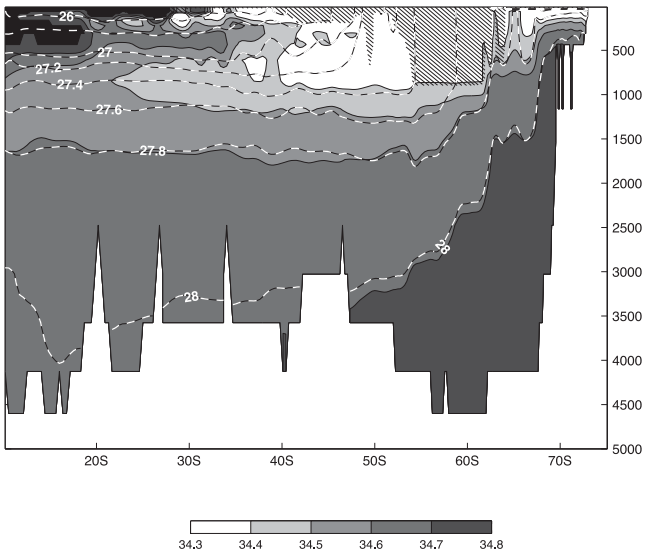

Figure 6. Salinity along a model late winter section through the eastern Pacific (along 80°W). Contours of neutral density are white, and the layers we define as deep mixed layers for this section are hatched.

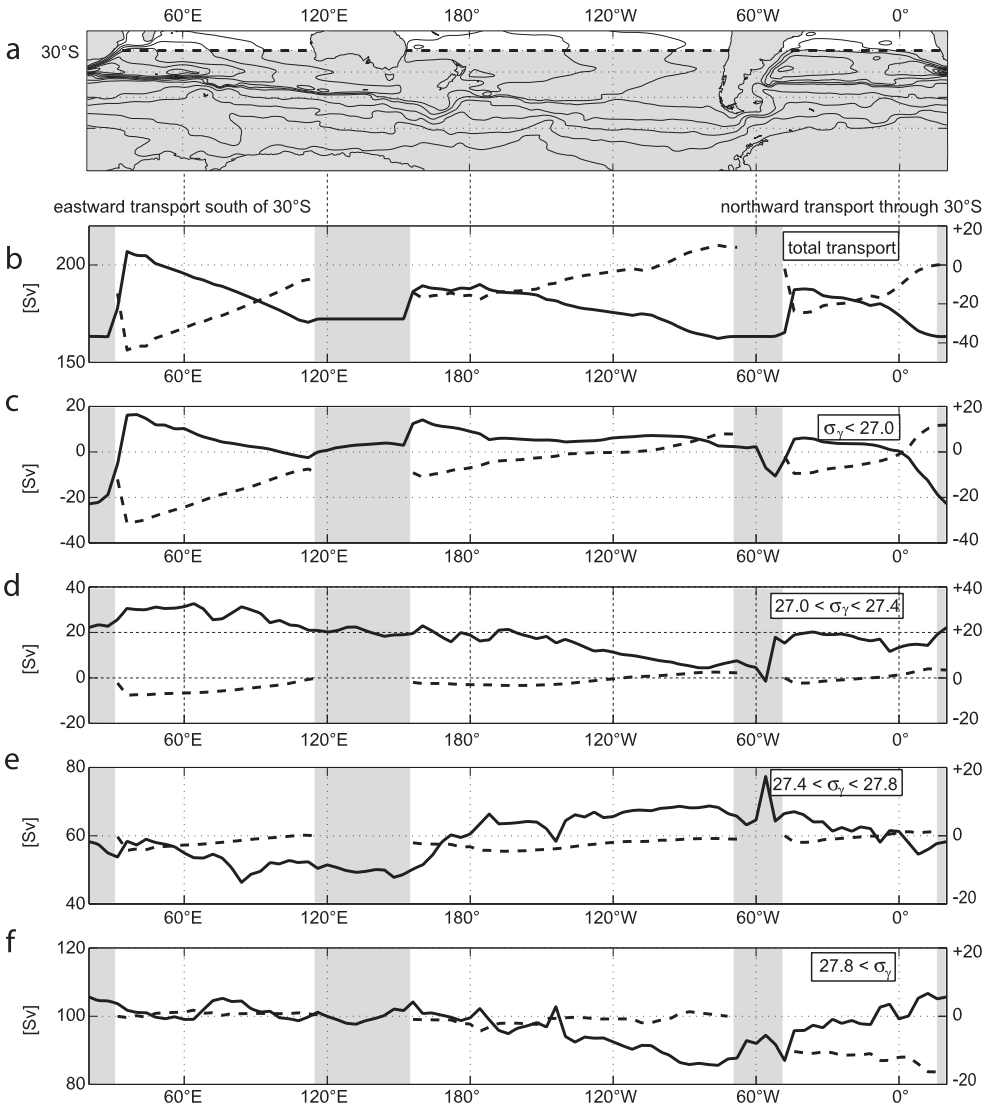

Figure 7. Zonal transport south of 30°S in the model (solid line, left vertical axis) and the meridional transport through 30°S accumulated per basin from the west (dashed line, right vertical axis). Positive values denote eastward (left side) and northward flow (right side).

position of the easternmost point in each basin indicates whether there is a net inflow from (when positive) or outflow into (when negative) the Southern Ocean within the respective density class. The dashed lines for the Indian and Pacific oceans in the total transport (Figure 7a) show a net transport to the south and north respectively, associated with the 10 Sv circulating around Australia and through the Indonesian passages. Note that the scales of the vertical axes are kept constant for both lines in a plot, resulting in seemingly small meridional transports, which may nonetheless be considerable.

[27] The fact that the gyre circulation and the circulation around Australia are contained mainly in the upper (lighter) range of the water column is reflected in the general similarity of the variations in the flow in the upper density interval ($\gamma_n < 27.0$) to that of the total flow (cf. Figures 7b and 7a). The surplus southward transport of warm water by the Agulhas current, which is not accounted for in the Indian Ocean but in the Pacific (dashed line), describes the circulation around Australia. A substantial part of this warmer, lighter Indian Ocean water (23 Sv) flows westward, enters the Atlantic where it contributes to the global overturning of North Atlantic Deepwater. South and southwest of Australia some of the lighter water is formed, notable as westward transport near 110°E, and an increase in eastward flow south of Australia (solid line). Around 150°E, the East Australian Current adds about 10 Sv of lighter water, most of which is lost (either to the north or to denser density classes) west of the date line.

[28] The major difference between Figures 7a and 7b (except for the mean) is that the 25 Sv decrease in the transport from 185 to 160 Sv along the Pacific part of the ACC that is seen in Figure 7a is not there in Figure 7b. The northward flow through 30°S into the Pacific is in the upper layer, but as very little of this lighter water enters the Pacific Ocean east of 190°E in the first place, it is replaced by newly formed light water. This is evident from the transport in the density range $27.0 < \gamma_n < 27.4$ (Figure 7c). This transport

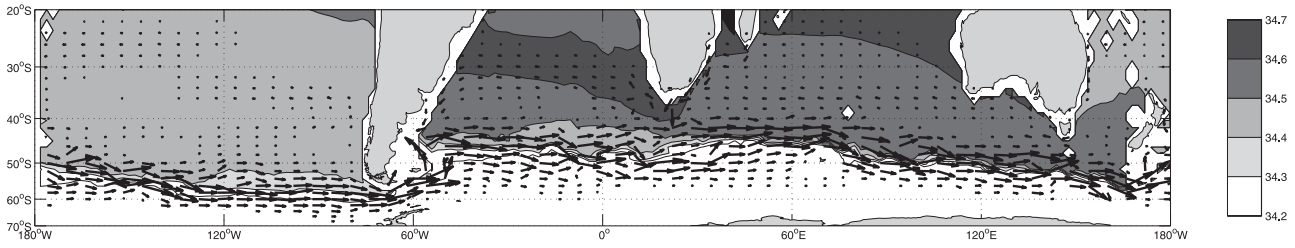

Figure 8. Mean model salinity at the γ_n = 27.4 neutral density level (contours). The transport in the density range $27.0 < \gamma_n < 27.8$ is depicted by vectors. The freshest AAIW is found in the Pacific. Salinity increases along the Atlantic and Indian parts of the ACC. Maximum salinity on the 27.4 density level is observed in the westward flowing limb of the South Atlantic subtropical gyre, where saline Indian Ocean water has leaked into the Atlantic.

is rather constant around 20 Sv, except for almost complete removal over the eastern part of the Pacific. Most of this loss is due to diapycnal transformation of intermediate density water to lighter densities. We will come back to this issue in the next section. In the Drake Passage region, there is diapycnal formation of about 20 Sv of this lighter variety of the Antarctic intermediate water in the model.

[29] The transport in the density range of the two AAIW components combined (so $27.0 < \gamma_n < 27.8$) is plotted on the mean salinity at the central γ_n = 27.4 level, to characterize the T/S development of the AAIW along the course of the ACC (Figure 8). The freshest water of this density is found in the south Pacific, and along the Atlantic and Indian Ocean sectors of the ACC salinification (and warming) is observed.

[30] The density layer $27.4 < \gamma_n < 27.8$ does not participate significantly in the gyre circulation, as there is little exchange between the subtropical basins and the Southern Ocean for this density class (dashed line in Figure 7d). The 12 Sv increase in the ACC transport in this density layer between eastern Australia and 180°E, without inflow from the north implies a divergence of the transport in this density layer, hence diapycnal formation. From these data, it is unclear what the formation mechanism is. For the deepest density class, $27.8 < \gamma_n$ (Figure 7e), the transport is reduced in the Pacific from around 100 Sv near 150°W to about 90 Sv near Drake Passage. This is indicative of diapycnal transformations, which should be analyzed with more detail than the four density classes permit.

2.3.2. Diapycnal Transformations

[31] Averaged over a sufficiently long period, convergence or divergence of the transport in an isopycnal layer can be interpreted as diapycnal removal or formation. As we determined the transports in isopycnal layers through the edges of 4° × 4° boxes, we can compute the diapycnal transformations in these boxes, and determine where net removal and formation of water masses within a certain density range occur. These transformations result from heat and freshwater fluxes at the surface and from diapycnal mixing. As in the model the lateral diffusion of tracers is in the horizontal plane, the latter may be substantial in regions of steeply sloping isopycnals. It is not a priori clear whether this is, at the present model resolution, a justifiable feature or an undesirable numerical artifact.

[32] We investigate first the transports through 30°S, which, together with the transport through the Indonesian passages, determine the diapycnal transformations of the three main ocean basins north of 30°S, and the Southern Ocean to the south.The mean transport through 30°S into the Atlantic in isopycnal layers (Figure 9), which can be interpreted as the convergence in those layers in the basin north of 30°S, shows convergence in the lighter layers and divergence in the denser layers. This implies a transformation from lighter to denser water in the Atlantic, consistent with a meridional overturning with formation of NADW in the North Atlantic. The Indian and Pacific curves denote the transports into the respective basins through 30°S, plus (for the Indian) or minus (for the Pacific) the Indonesian Throughflow. The Southern Ocean curve is the negative of the sum of the three, and can be interpreted as the convergence in isopycnal layers in the Southern Ocean. These results closely agree with those presented by *Talley* [2003], which are based on hydrographic observations. Most of the transports founds by *Talley* [2003] are comparable to those found in an inversion experiment by *Sloyan and Rintoul* [2001a]. For example, the 16.7 Sv of NADW exported from the Atlantic agrees fully with 17.8 Sv in the work by *Talley* [2003] and 17 Sv in the work by *Sloyan and Rintoul* [2001b]. An exception is the Indian Ocean, where [*Talley*, 2003] finds an intermediate level overturning of 10.7 Sv of deep to intermediate upwelling,whereas [*Sloyan and Rintoul*, 2001b] give a much larger estimate for this overturning (20 Sv). Our estimate of 10.5 Sv agrees well with that of *Talley* [2003].

[33] The isopycnal transformations reflect the thermodynamic differences between the midlatitude oceans and the Southern Ocean (Figure 9). 16.7 Sv of North Atlantic Deepwater (NADW) flows out of the Atlantic into the Southern Ocean, and is replaced by northward flow of thermocline and intermediate waters. The water lighter than 26.2 is derived from the Indian Ocean. These waters are quickly cooled in the Atlantic, adding to the intermediate density waters that are exported further northward. The denser waters are mostly derived from the Drake Passage, and either circulate through the Indian Ocean subtropical gyre or enter the South Atlantic gyre in the highly variable region near South Africa [*Gordon et al.*, 1992] (see also Figure 8). Both routes involve transformations toward lower densities and higher salinities by mixing with warm and saline Indian Ocean subtropical water.

[34] The Indian Ocean exports rather light (warm) intermediate and thermocline waters in the density range 25.0–

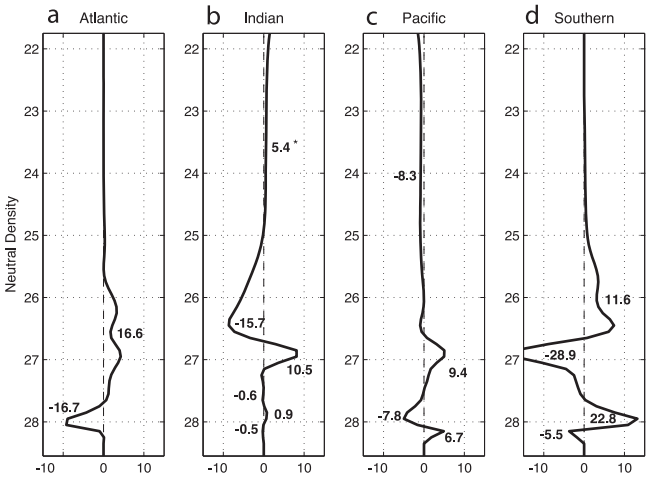

Figure 9. Model transports in isopycnal layers into each of the four major ocean basins through 30°S, where the Atlantic, Indian, and Pacific oceans are defined as the respective basins north of 30°S. These transports can be interpreted as diapycnal transformations within the basins. A net inflow (outflow) implies that the density class loses (gains) volume within the basin. Sums over adjacent density intervals with net convergence/divergence are added as bold numbers. The units on the horizontal axis correspond to convergence within 0.1 neutral density ranges (Sv). A small (0.5 Sv) correction was applied to the Indonesian Throughflow to correct for a miscalculation. Part of this correction may have occurred in the density classes below $\gamma_n = 25$, so the divergence in the upper density classes may range between 4.9 and 5.4 Sv, and that in the intermediate classes is between −15.7 and 15.2 Sv.

26.8 (Figure 9b). These waters provide heat to the Southern Ocean through southward eddy heat transport along the southern boundary of the gyre, and provide the warm waters that enter the Atlantic. This large export of heat from the Indian Ocean is facilitated by an inflow of warm tropical Pacific waters through the Indonesian passages (ITF). The model simulates a westward throughflow of 9 Sv in the density classes $\gamma_n < 26.8$, which together with 10.5 Sv of denser intermediate waters form the exported 15.7 Sv warm intermediate and thermocline water. Southward transport of this warm ITF water in the Ekman layer [e.g., *Song et al.*, 2004] (and probably to a lesser extent in the Leeuwin Current along the Australian west coast) leads to the relatively strong cooling observed over the South Indian Ocean subtropical gyre. *Talley* [2003] chooses the Agulhas outflow for the ITF such, that a small southward heat flux remains associated with the ITF circulation, which implies a slight warming of the ITF water during its passage through the Indian Ocean. From our model analysis and the results presented by *Song et al.* [2004], a significant heat loss from the ITF over the South Indian gyre is expected. This would imply a stronger southward heat transport in the Agulhas Current associated with the gyre circulation. Such interpretation leaves the total heat transports unchanged, but offers an alternative view of the role off the ITF water in the heat transport of the South Indian Ocean, and is consistent with the observations that little is left of the ITF water mass signature in the western part of the basin [*Talley and Sprintall*, 2004].

[35] The Pacific limb of the ITF circulation around Australia is reflected in the diapycnal transformations by the transformation of 9.4 Sv of intermediate waters, most of which (8.3 Sv) goes into lighter density classes (Figure 9c). The Pacific is the only basin that shows a deep overturning cell of Antarctic Bottom water (AABW). Approximately 6.7 Sv of AABW enters the Pacific, and is converted into lighter Antarctic circumpolar deepwater, although the model results are not reliable in this density range as was discussed in the introduction.

[36] The Southern Ocean facilitates the interocean exchange of water masses [*Speer et al.*, 2000; *Webb and Suginohara*, 2001; *Sloyan and Rintoul*, 2001b]. Figure 9d shows the two-cell overturning in the Southern Ocean, with export of the AABW (5.5 Sv) and waters in the intermediate density range (28.9 Sv in the range $26.6 < \gamma_n < 27.6$). The latter are formed out of North Atlantic deep water and Antarctic circumpolar deep water (22.8 Sv) and surface and thermocline waters (11.6 Sv). The Southern Ocean water mass transformations are not uniformly distributed around the ACC (Figure 7). The Pacific sector of the ACC south of 30°S (between southeastern Australia at 150°E and Drake Passage) is the region where the coldest, densest waters ($\gamma_n \approx 28.0$) are formed (Figure 10). The strongest formation of the denser part of the AAIW in the model ($27.4 < \gamma_n < 27.8$) occurs between Australia and the Campbell Plateau near New Zealand (Figure 7).

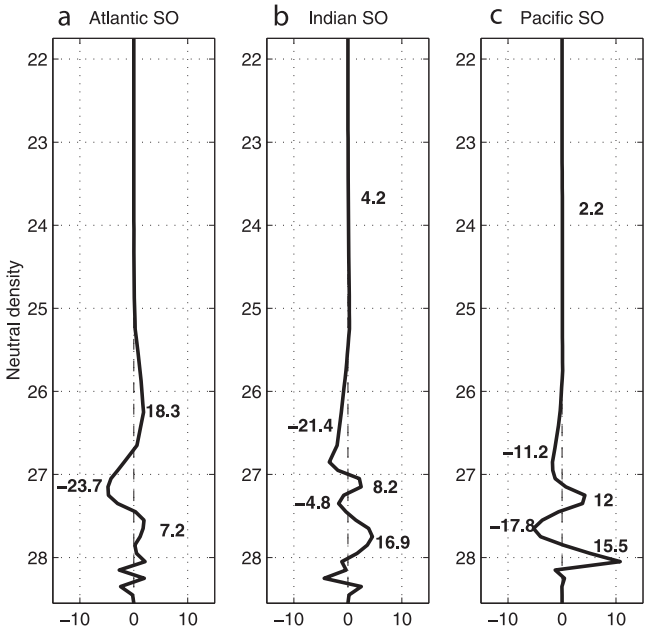

Figure 10. As in Figure 9, but here the Southern Ocean transformations (Figure 9d) are divided into transformations in the parts of the Southern Ocean south of the respective oceans and are divided by the Drake Passage and the meridians through the southernmost points of Africa (near 20°E) and Australia/Tasmania (near 150°E). For example, the Figure 9a (Atlantic SO) shows transformations within the Southern Ocean south of 35°S and between Drake Passage and 20°E.

[37] The Indian sector of the Southern Ocean gains buoyancy over most density ranges: 21.4 Sv of light intermediate and thermocline waters are formed out of mostly denser intermediate waters. The Indian sector of the Southern Ocean produces water in very similar density classes as the subtropical Indian Ocean ($\gamma_n < 26.8$), but does so by removing denser waters, mostly those in the Pacific AAIW range.

[38] The main production sites for the lighter AAIW density classes are found in the Atlantic, where 24 Sv of intermediate water ($26.8 < \gamma_n < 27.4$) is formed (Figure 10a). A large portion of this water is formed out of even lighter water, by cooling and mixing of warm subtropical water carried south by the Agulhas and South Brazil Currents. The dissipation of Agulhas rings and the strong mixing in the Brazil-Malvinas confluence zone are the primary places of water mass transformation in the South Atlantic. However, the diapycnal formation of water in the AAIW density class is not the only important factor in determining the formation of AAIW: in the southeast Pacific, there may be no net formation of water in this density class, but the temperature and salinity properties of the water may be strongly altered: the jump in T/S characteristics on the AAIW level between the Indian and Pacific oceans [*McCartney*, 1977] (see also Figure 8) suggests that this is the case. *Sloyan and Rintoul* [2001a] find strong diapycnal fluxes across both the upper- and lower-density levels bounding the AAIW, with very little net volume change of the layer in between, but significant changes in T/S properties.

3. Mechanisms

[39] To elucidate the diapycnal processes involved in the formation of mode and intermediate waters in the Southern Ocean, we investigated the contributions of air-sea interaction and eddy-induced heat and density fluxes.

[40] In the region around the Subantarctic front, Ekman transport leads to a displacement of southern waters across the front. These cool (though fresh) waters lead to reduced or unstable stratification, which favors convection north of the front. Ekman forcing can also lead to preconditioning of the water column by upwelling, favoring convection in winter when the surface is cooled. Variability in the northward Ekman flow of relatively cool and fresh surface water modifies the characteristics of the AAIW, as has been found in observations [*Rintoul and England*, 2002] as well as coarse resolution models [*Santoso and England*, 2004]. Eddy heat fluxes are of considerable magnitude in the Southern Ocean and generally oppose the heat flux induced by the mean flow [*De Szoeke and Levine*, 1981; *Wunsch*, 1999]. Estimates range between 0.3 and 0.9 PW (PW = 10^{15} W) [e.g., *Gille*, 2003, and references therein]. Although both the atmospheric fluxes and the variability of the ocean itself are poorly sampled both in time and space, the southward heat flux by eddies through the ACC is a robust result of various independent techniques. Eddy fluxes of heat and salt have been proposed as the main factor in setting the transport and stratification of the ACC [*Karsten et al.*, 2002]. In the following paragraphs, we will discuss three of the mechanisms that together result in the formation of AAIW, namely, air-sea fluxes (section 3.1), the effect of the mean flow and Ekman transport (section 3.2), and the role of eddy fluxes across the ACC (section 3.3).

3.1. Air-Sea Fluxes

[41] In this analysis, we assume that the air-sea fluxes that act on surface of the ocean are distributed downward over the depth of the mixed layer. We use the monthly mean mixed layer depths derived from the POCM model as defined in section as the depth interval on which the fluxes act. For stratified cases, we use a minimum mixed layer depth of 50 m. The model is forced by ECMWF fluxes of heat and freshwater, and by a modest restoring toward climatology. Our use of the Comprehensive Ocean Atmosphere Data set (COADS) data set is thus not consistent with the POCM model forcing, and should not be regarded quantitatively. Rather, we use this analysis to assess the importance of surface forcing for the diapycnal fluxes in the upper layers of the model, and to evaluate the geographical inhomogeneity of this diapycnal forcing. For this, the COADS data set is appropriate, although it should be kept in mind that *Sloyan and Rintoul* [2001a] find considerable differences in the diapycnal fluxes, resulting from the use of different forcing climatologies. The monthly mean mixed layer depths were computed as the climatologically averaged mixed layer depths, with months centered on the first day of each month to obtain average initial conditions for the month. The same averages for sea surface temperature and salinity were obtained from the model output (T_0 and S_0). These initial conditions are then acted upon by the surface fluxes from the COADS data set, Q_h for heat flux (Watt) and Q_{fw} for fresh water flux (m/s).

[42] The resulting temperature and salinity at the end of the month (T_1 and S_1) are computed as

$$T_1 = T_0 + \frac{Q_h T}{h_{ml}\,\rho_0\,C_p},\quad S_1 = \frac{S_0\,h_{ml}}{h_{ml} + Q_{fw} T},$$

where h_{ml} is the mixed layer depth, ρ_0 the initial density, T the length of a month, and C_p the heat capacity of seawater. Diapycnal transformations are defined as changes in density due to these changes in temperature and salinity: $\gamma_n^0 = \gamma_n(T_0, S_0)$ and $\gamma_n^1 = \gamma_n(T_1, S_1)$.

[43] The diapycnal convergence in a density range $\gamma_n \in [\gamma_n^0, \gamma_n^1]$ over an area A is then for each month defined as the difference between the area integrals at the end (t = 1) and beginning (t = 0) of the month:

$$C = \iint h_{ml}\,\delta(\gamma_n)\,dA\;\Big|_{t=1}^{t=0},$$

where $\delta(\gamma_n) = 1$ for $\gamma_n(x, y) \in [\gamma_n^0, \gamma_n^1]$ and 0 elsewhere. Summed over a year for the whole Southern Ocean this yields a large formation of waters in the range $26.8 < \gamma_n < 27.4$, the lighter half of the Antarctic intermediate water range (Figure 11). This water is formed out of the denser AAIW range ($27.4 < \gamma_n < 27.8$), mostly due to the heat flux into the ocean. Most of these conversions are located in the Indian Ocean, with small contributions from the western Pacific sector west of 160°W, and the Atlantic sector. The central and eastern Pacific are regions of very small

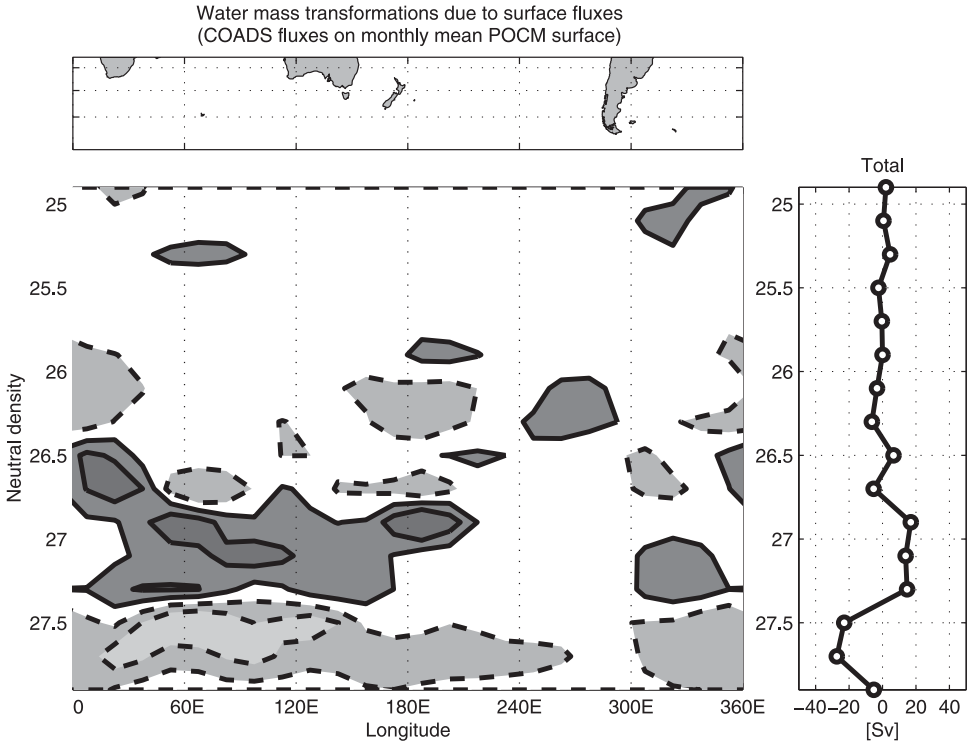

Figure 11. Diapycnal transformations due to surface forcing of heat and freshwater. In the bottom left plot, we divide the Southern Ocean diapycnal transfers into 24 sectors 15° wide to be able to geographically locate the main regions of diapycnal transformations. The ocean south of 30°S is considered, and the total (zonally integrated) is plotted in the right plot. Positive values denote formation (divergence) in that neutral density class.

diapycnal fluxes due to surface forcing. These results are consistent with those of *Speer et al.* [2000] and *Sloyan and Rintoul* [2001b], who concluded that most of the diapycnal transformations induced by surface fluxes are located in the Indian sector of the Southern Ocean.

3.2. Mean Flow/Ekman Contribution

[44] To assess the mean contribution of eddy fluxes to the water mass transformations in the Southern Ocean, we adopted a reference frame that follows the stream function contours of the vertically integrated circulation of the Southern Ocean (Figure 1). This avoids the problems associated with the zonally averaged framework outlined by *Döös and Webb* [1994]. Experiments with contours of the mean sea surface height, which may be a closer approximation of geostrophic contours for the upper ocean circulation, gave very similar results for the eddy fluxes and are not included in this paper.

[45] The eddy fluxes were calculated across 13 circumpolar contours of the stream function. In these calculations, the 40 and 160 Sv contours mark the approximate southern and northern boundaries of the ACC (Figure 1). The mean latitudes of these contours range between 49°S and 60°S, although locally they can extend from 43°S to south of 70°S.

[46] The mean meridional stream function of the transport across these contours (Figure 12) shows a strong northward Ekman transport in the upper layer of the model. It increases

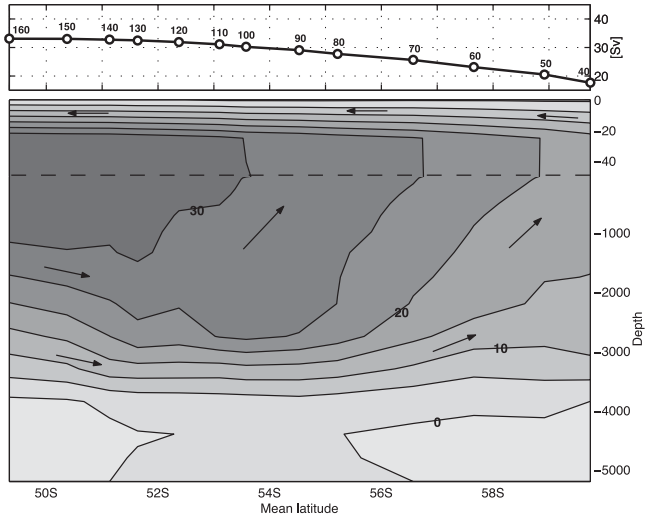

Figure 12. Vertical stream function of the meridional flow across the ACC contours in the model. Along the horizontal axis are the mean latitudes of the stream function contours of the vertically integrated stream function (Figure 1). Contours here are every 5 Sv, and the upper 50 m of the vertical axis are exaggerated. The small top plot shows the Ekman transport across the contours, as defined by the shear in the upper 50 m of the model. The increase in northward Ekman transport drives 17 Sv of upwelling over the ACC region.

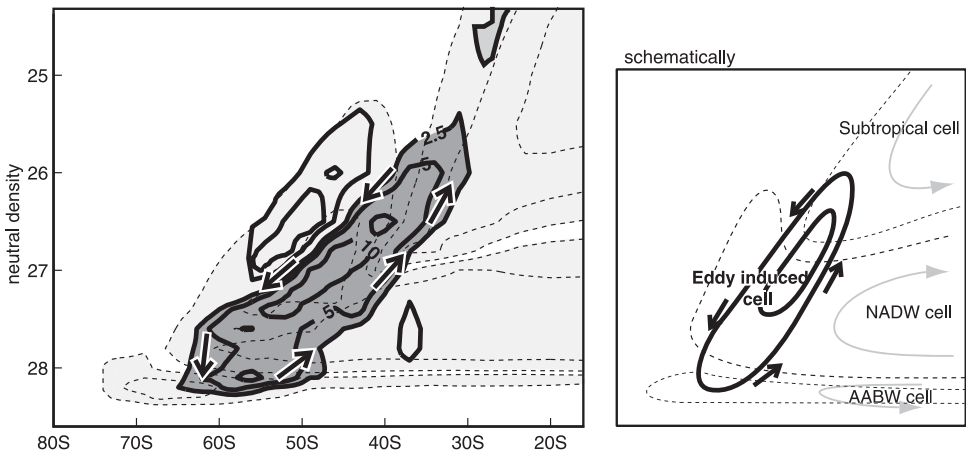

Figure 13. (left) Eddy-induced component of the zonally integrated meridional overturning in neutral density coordinates for the oceans south of 20°S. The total overturning repeated from Figure 2 is shown with dashed lines to link the location of the main eddy-induced overturning cells to the general circulation. Negative stream function values (shaded gray) denote anticlockwise circulation. (right) Schematic representation of the eddy-induced component.

from 17 Sv across the southernmost (40 Sv) contour, to 33 Sv across the northernmost (160 Sv), with an associated upwelling across the ACC of 17 Sv. The return flow of 33 Sv is uniformly distributed over the upper 4000 m of the model domain. This mean flow implies a northward flux of heat and southward flux of salt. The net northward heat flux by the mean circulation and the loss of heat to the atmosphere in the Southern Ocean is compensated for by a southward eddy heat flux that locally exceeds the northward heat flux of the mean flow. The southward salt flux of the mean flow is consistent with the atmospheric forcing of a considerable freshwater flux into the ocean. It should be noted that most of the interior flow (below the Ekman layer) is located on the eastern flanks of the major topographic features, most notably South America.

3.3. Eddy Fluxes

[47] We calculate the eddy fluxes for tracers as the residual between the mean tracer transport and the transport of the mean tracer by the mean currents. The effect of the eddies on the zonally integrated meridional overturning (the total is shown in Figure 2) is considerable (Figure 13). There is a strong (13 Sv) counterclockwise cell between 30°S and 60°S, which transports relatively light water to the south, and replaces it with denser water. The dashed lines in Figure 13 show the total overturning, and the position of the eddy-induced circulation relative to it. The eddy driven circulation facilitates the exchange between the subtropical gyres and the ACC. As the eddy-induced cell crosses the density range in which the intermediate waters are formed and exported to the subtropical basins, the exchange of water by eddies, and their subsequent dissipation and mixing seems to be an important factor in the formation of intermediate waters at the boundary between the gyres and the ACC. To further investigate the eddy driven circulation, we evaluated the total mean fluxes and fluxes of the mean fields as defined before. The heat fluxes associated with the mean fields, the eddy component and the combined total for the POCM model are all within the range of values previously reported (Figure 14). (See *Gille* [2003] for an overview of observations.)

[48] The oceanic heat flux by mean fields is small in the southernmost part, but northward over the complete ACC stream function range, and increases in northward direction

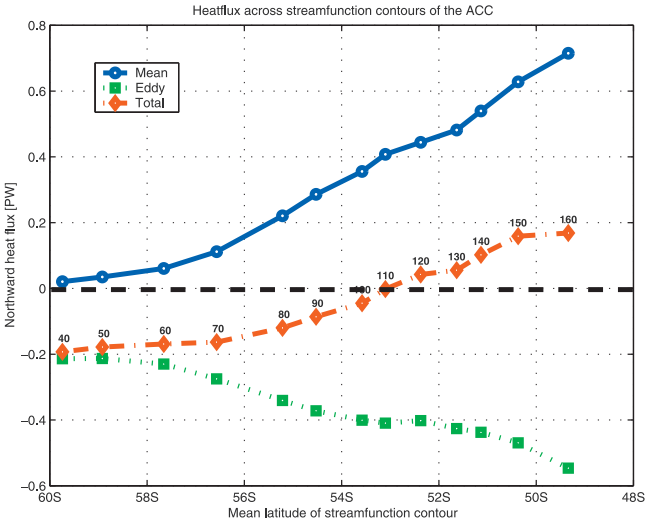

Figure 14. Heat fluxes by the mean flow (solid line) and by the eddies (dotted line) and their total (dash-dotted line) across the stream function contours of the ACC (Figure 1). The stream function values used (between 40 and 160 Sv from south to north across the ACC) are included along the dash-dotted line. As the horizontal coordinate, we have used the mean latitude of the stream function contour. The "total" ocean heat flux mirrors the atmospheric heat flux: South of the 110 Sv contour (53°S), the ocean loses heat to the atmosphere. This is facilitated by a southward eddy heat flux that is stronger than the northward heat flux by the mean flow.

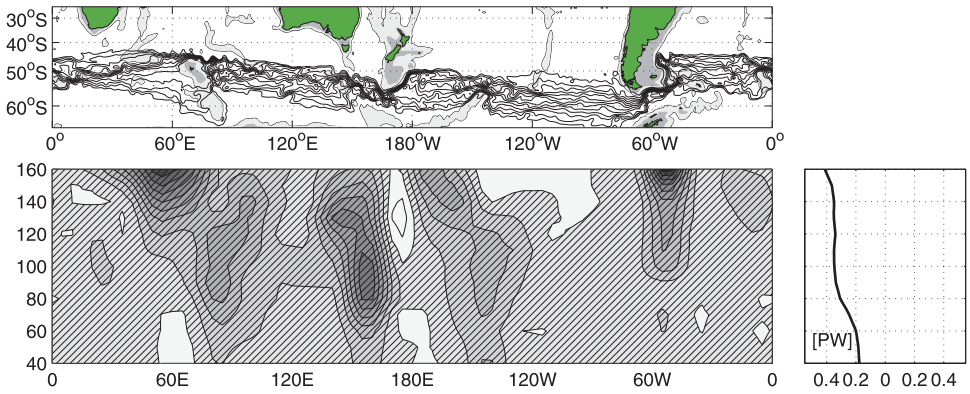

Figure 15. Eddy heat flux across the contours of the vertically integrated stream function (vertical axes). Southward fluxes are dashed. The plot to the right shows the integrated eddy fluxes around the ACC contours (as in Figure 14). The strongest southward eddy heat fluxes occur at the Brazil/Malvinas confluence in the Atlantic and along the path of the Agulhas Return Current.

up to around 0.7 PW for the northern boundary of the ACC. This increase is partly due to the increasing temperatures of the northward Ekman transport and the increasing portion of the meridional overturning (Figure 12). *De Szoeke and Levine* [1981] estimated an Ekman transport through a circumpolar path near the Subantarctic front of 28 Sv and an associated equatorward heat flux of 0.15 PW. They found that the total geostrophic heat flux was indistinguishable from zero, which, combined with an estimated warming south of the front by 0.3 PW led to an estimated 0.45 PW southward eddy heat transport. Our "mean flow" component includes both the Ekman component and a substantial baroclinic component which is not necessarily limited to the deep ocean (Figure 12), as the stream function contours meet shallow topography in the Drake Passage, and at the Kerguelen and Campbell Plateaus (Figure 1).

[49] The southward heat transport in the southern part of the ACC is achieved by an eddy heat flux of 0.2 PW. For the northern part of the ACC, the southward eddy heat flux increases to 0.45 PW for the northernmost ACC contours. The agreement between the estimates of *De Szoeke and Levine* [1981] and our calculations might be coincidental, since their estimate of the atmospheric heat flux of 0.3 PW seems to be quite different from that forcing the POCM model (0 PW for the 110 Sv contour, and between −0.2 PW and +0.2 PW for the others; see Figure 14).

[50] The eddy fluxes of heat, freshwater and buoyancy are not homogeneously distributed around the ACC contours. We have separated the mean, total and eddy fluxes in 15° zonal sectors of the ACC contours, showing several locations of strongly increased eddy heat fluxes (Figure 15). The eddy buoyancy flux is dominated by the heat flux.

[51] The heat flux, albeit negative (southward) over almost the complete ACC, shows several "hot spots" for eddy heat input from the gyres to the north. The main regions for eddy heat input are along the Agulhas Return Current (20°–70°E), in the Brazil-Malvinas Confluence region (60°–40°W), and to a lesser extent east of New Zealand. Southward of these locations the imported heat is transported further south across the ACC while being advected east by the current itself, resulting in the slanted areas of enhanced southward heat flux. South of Australia, heat is transported southward across the ACC by eddies.

4. Conclusions

[52] We have investigated the Southern Ocean of an intermediate/high resolution ocean general circulation model (the POCM) for the main pathways, formation sites and mechanisms of formation and modification of intermediate water. The POCM seems reasonably successful in simulation the vertically integrated flow, and the diapycnal overturning of the Southern Ocean. These quantities are mostly in agreement with current understanding, both from observations or from other ocean models for the surface and intermediate layers. The deepest water mass observed in the real ocean, the Antarctic Bottom water is not simulated well in the POCM because of the absence of Antarctic shelf processes limiting its formation, and the crudeness of the deep topography limiting its northward spreading into the midlatitude oceans through narrow channels. The northward transport of intermediate waters into the South Atlantic, which compensates for the export of North Atlantic deep-water, is mostly in the lighter neutral density ranges ($\gamma_n <$ 27.4).

[53] The temporal and spatial characteristics of mode water formation were diagnosed from the simulated deep winter mixed layers, and seem to be mostly in agreement with observations. The notable exception is the density of newly formed Antarctic intermediate water in the southeast Pacific, where mode waters are formed at denser levels than seems to be the case in reality. Modeled deep winter mixed layers seem to be deeper than realistic in that part of the ocean. The diapycnal formation of the $27.4 < \gamma_n <$ 27.8 density class that is involved in this mode water formation takes place in the western Pacific. It is also this water mass that forms the bulk of the intermediate water transported through Drake Passage. The traditional AAIW density class of $27.0 < \gamma_n < 27.4$ is formed mostly in the Atlantic, due to mixing of the cooler waters formed in the Pacific with warmer surface and thermocline waters in the Brazil-Malvinas Confluence and the Agulhas Retroflection regions. The northward transport of intermediate

waters into the South Atlantic, which compensates for the export of North Atlantic deepwater, is mostly in the lighter density ranges (γ_n < 27.4). The northward transport of intermediate waters into the South Atlantic, which compensates for the export of North Atlantic deepwater, is mostly in the lighter density ranges (above 27.4). This supports the view that the water from Drake Passage that flows northward through the South Atlantic is modified first through mixing in the combined South Indian/Atlantic circulation [*Gordon et al.*, 1992].

[54] The total mean fluxes of heat and salt across the ACC contours are set by the atmosphere-ocean fluxes prescribed to the model. The division of this prescribed flux into a mean and eddy component is not prescribed. An underdeveloped eddy field will lead to adjustments in the fluxes resulting from the mean fields, as in that case diffusion has to provide the fluxes. The only way to get the mean fields into a realistic range is thereby to also model the eddy characteristics in a manner that consistent with the real ocean. The total, mean field, and eddy heat fluxes across the ACC contours in the POCM model seem to fall within our range of current knowledge. It is reassuring to see that, although the model is only on the verge of resolving eddy processes, it seems to capture the fluxes associated with the eddying nature of the real ocean.

[55] Air/sea fluxes seem to be of minor importance in the diapycnal modification of water masses over most of the Southern Ocean. The Indian Ocean sector is the clear exception, as up to 45 Sv of intermediate water is formed out of denser water in that part of the ocean because of surface warming and precipitation. It should be noted, however, that our computations are not fully consistent with the fluxes applied to the model, and can only be considered a rough estimate of the relative importance of air/sea fluxes in the density transformations in different parts of the Southern Ocean. As *Sloyan and Rintoul* [2001a] show, Southern Ocean fluxes are rather poorly defined and differ substantially between climatologies. Also, the effects of heat and freshwater fluxes may cancel and substantially modify the water mass characteristics without changes in density.

[56] The effect of eddy fluxes on formation and distribution of intermediate water in the Southern Ocean cannot be explicitly inferred from these analyses. However, we have shown that the eddies play a major role in the exchange of water masses between the midlatitude gyres and the Southern Ocean. It is this exchange, and the subsequent dissipation and mixing of the exchanged waters, that eventually leads to the formation of intermediate density waters. The strong zonal inhomogeneity of the eddy fluxes is one of the factors determining the nature of the final result: the mode waters formed in the eastern Pacific are the furthest away from sources of heat input into the ACC, and thereby likely to produce the coldest mode waters. The fact that it is the furthest south, and thereby prone to the coldest overlying atmosphere, may be important in setting the conditions for winter deep mixing and determining the T/S characteristics, but does not seem to be the main factor in the diapycnal formation of these waters. However, observations of air/sea interaction in the southeast Pacific are sparse, and new observations may provide better estimates of the induced fluxes and their role in the formation of AAIW.

[57] **Acknowledgments.** This work was supported by NSF grant OCE0118363, NASA grant NAG512378, and JPL contract 1206714. We thank I. M. Belkin and the anonymous reviewers for their efforts and extensive comments and insightful suggestions and Robin Tokmakian (Naval Postgraduate School, Monterey, California) for kindly providing us with the POCM model output.

References

Beal, L. M., and H. L. Bryden (1999), The velocity and vorticity structure of the Agulhas Current at 32°S, *J. Geophys. Res.*, *104*, 5151–5176.

Belkin, I. M., and A. L. Gordon (1996), Southern Ocean fronts from the Greenwich meridian to Tasmania, *J. Geophys. Res.*, *101*, 3675–3696.

Byrne, D. A., A. L. Gordon, and W. F. Haxby (1995), Agulhas eddies: A synoptic view using Geosat ERM data, *J. Phys. Oceanogr.*, *25*, 902–917.

Chaigneau, A., and O. Pizarro (2005), Surface circulation and fronts of the South Pacific Ocean, east of 120°W, *Geophys. Res. Lett.*, *32*, L08605, doi:10.1029/2004GL022070.

Chiswell, S. M., J. Toole, and J. Church (1997), Transports across the Tasman Sea from WOCE repeat sections: The East Australian Current 1990–94, *N. Z. J. Mar. Freshwater Res.*, *31*, 475–479.

De Ruijter, W. P. M. (1982), Asymptotic analysis of the Agulhas and Brazil Current systems, *J. Phys. Oceanogr.*, *12*, 361–373.

De Ruijter, W. P. M., A. Biastoch, S. S. Drijfhout, J. R. E. Lutjeharms, R. P. Matano, T. Pichevin, P. J. van Leeuwen, and W. Weijer (1999), Indian-Atlantic interocean exchange: Dynamics, estimation and impact, *J. Geophys. Res.*, *104*, 20,885–20,910.

De Szoeke, R. A., and M. D. Levine (1981), The advective flux of heat by mean geostrophic motions in the Southern Ocean, *Deep Sea Res., Part A*, *28*, 1057–1085.

Döös, K., and D. J. Webb (1994), The Deacon cell and other meridional cells of the Southern Ocean, *J. Phys. Oceanogr.*, *24*, 429–442.

England, M. H. (1993), Representing the global-scale water masses in ocean general circulation models, *J. Phys. Oceanogr.*, *23*, 1523–1552.

England, M. H., J. S. Godfrey, A. C. Hirst, and M. Tomczak (1993), The mechanism for Antarctic intermediate water renewal in a world ocean model, *J. Phys. Oceanogr.*, *23*, 1553–1560.

Ganachaud, A., C. Wunsch, J. Marotzke, and J. Toole (2000), The meridional overturning and large scale circulation of the Indian Ocean, *J. Geophys. Res.*, *105*, 26,117–26,134.

Gent, P. R., and J. C. McWilliams (1990), Isopycnal mixing in ocean circulation models, *J. Phys. Oceanogr.*, *20*, 150–155.

Gille, S. T. (1997), The Southern Ocean momentum balance: Evidence for topographic effects from numerical model output and altimeter data, *J. Phys. Oceanogr.*, *27*, 2219–2232.

Gille, S. T. (2003), Float observations of the Southern Ocean. part II: Eddy fluxes, *J. Phys. Oceanogr.*, *33*, 1182–1196.

Gordon, A. L., D. T. Georgi, and H. W. Taylor (1977), Antarctic polar front zone in the western Scotia Sea, *J. Phys. Oceanogr.*, *7*, 309–328.

Gordon, A. L., et al. (1992), Thermocline and intermediate water communication between the South Atlantic and Indian oceans, *J. Geophys. Res.*, *97*, 7223–7240.

Gregory, J. M. (2000), Vertical heat transports in the ocean and their effect on time-dependent climate change, *Clim. Dyn.*, *16*, 501–515.

Hanawa, K., and L. D. Talley (2001), Mode waters, in *Ocean Circulation and Climate*, *Int. Geophys. Ser.*, edited by G. Siedler, J. Church, and J. Gould, pp. 373–386, Elsevier, New York.

Jayne, S., and J. Marotzke (2001), The dynamics of ocean heat transport variability, *Rev. Geophys.*, *39*, 385–411.

Karsten, R., H. Jones, and J. Marshall (2002), The role of eddy transfer in setting the stratification and transport of a circumpolar current, *J. Phys. Oceanogr.*, *32*, 39–54.

Matano, R., and E. Beier (2003), A kinematic analysis of the Indian/Atlantic interocean exchange, *Deep Sea Res., Part II*, *50*, 229–249.

McCarthy, M. C., and L. D. Talley (1999), Three-dimensional isoneutral potential vorticity structure in the Indian Ocean, *J. Geophys. Res.*, *104*, 13,251–13,267.

McCartney, M. S. (1977), Subantarctic mode water, in *A Voyage of Discovery: George Deacon 70th Anniversary Volume*, edited by M. Angel, pp. 103–119, Elsevier, New York.

McCartney, M. S. (1982), The subtropical recirculation of mode waters, *J. Mar. Res.*, *40*, suppl., 427–464.

Molinelli, E. J. (1981), The Antarctic influence on Antarctic intermediate water, *J. Mar. Res.*, *39*, 267–293.

Patterson, S. L., and T. Whitworth (1990), Physical oceanography, in *Antarctic Sector of the Pacific*, edited by G. Glasby, pp. 55–93, Elsevier, New York.

Peterson, R., and L. Stramma (1991), Upper level circulation in the South Atlantic Ocean, *Prog. Oceanogr.*, *25*, 1–73.

Piola, A. R., and A. L. Georgi (1982), Circumpolar properties of Antarctic intermediate water and Subantartic mode water, *Deep Sea Res., Part A*, *29*, 687–711.

Piola, A. R., and A. L. Gordon (1989), Intermediate water in the southwest South Atlantic, *Deep Sea Res., Part A*, *36*, 1–16.

Rintoul, S. R., and M. H. England (2002), Ekman transport dominates local air-sea fluxes in driving variability of Subantarctic mode water, *J. Phys. Oceanogr.*, *32*, 1308–1321.

Santoso, A., and M. H. England (2004), Antarctic intermediate water circulation and variability in a coupled climate model, *J. Phys. Oceanogr.*, *34*, 2160–2179.

Schouten, M. W., W. P. M. de Ruijter, P. J. van Leeuwen, and J. R. E. Lutjeharms (2000), Translation, decay and splitting of Agulhas rings in the south-east Atlantic Ocean, *J. Geophys. Res.*, *105*, 21,913–21,925.

Sloyan, B., and S. Rintoul (2001a), Circulation, renewal and modification of Antarctic mode and intermediate water, *J. Phys. Oceanogr.*, *31*, 1005–1030.

Sloyan, B., and S. R. Rintoul (2001b), The southern ocean limb of the global deep overturning circulation, *J. Phys. Oceanogr.*, *31*, 143–173.

Song, Q., A. L. Gordon, and M. Visbeck (2004), Spreading of the Indonesian throughflow in the Indian Ocean, *J. Phys. Oceanogr.*, *34*, 772–792.

Sorensen, J. V., J. Ribbe, and G. Shaffer (2001), Antarctic intermediate water mass formation in ocean general circulation models, *J. Phys. Oceanogr.*, 3295–3311.

Speer, K., S. R. Rintoul, and B. Sloyan (2000), The diabatic Deacon cell, *J. Phys. Oceanogr.*, *30*, 3212–3222.

Speich, S., B. Blanke, and G. Madec (2001), Warm and cold water routes of an O. G. C. M. thermohaline conveyor belt, *Geophys. Res. Lett.*, *28*(2), 311–314.

Stammer, D., R. Tokmakian, A. Semtner, and C. Wunsch (1996), How well does a 1/4° global circulation model simulate large-scale oceanic observations?, *J. Geophys. Res.*, *101*, 25,779–25,812.

Stramma, L., and J. R. E. Lutjeharms (1997), The flow of the subtropical gyre of the South Indian Ocean, *J. Geophys. Res.*, *102*, 5513–5530.

Talley, L. (2003), Shallow, intermediate and deep overturning componenets of the global heat budget, *J. Phys. Oceanogr.*, *33*, 530–560.

Talley, L. D., and J. Sprintall (2004), Deep expression of the Indonesian Throughflow: Indonesian Intermediate Water in the South Equatorial Current, *J. Geophys. Res.*, *110*, C10009, doi:10.1029/2004JC002826.

Tokmakian, R., and P. G. Challenor (1999), On the joint estimation of model and satellite sea surface height anomaly errors, *Ocean Modell.*, *1*, 39–52.

Tsuchiya, M., and L. D. Talley (1996), Water-property distributions along an eastern Pacific hydrographic section at 135W, *J. Mar. Res.*, *54*, 541–564.

Webb, D. J., and N. Suginohara (2001), Vertical mixing in the ocean, *Nature*, *409*(6816), 37.

Whitworth, T., and W. D. Nowlin Jr. (1987), Water masses and currents of the Southern Ocean at the Greenwich meridian, *J. Geophys. Res.*, *92*, 6462–6476.

Wijffels, S. E., R. W. Schmidt, H. L. Bryden, and A. Stigebrandt (1992), Transport of freshwater by the oceans, *J. Phys. Oceanogr.*, *22*, 156–162.

Wunsch, C. (1999), Where do ocean eddy heat fluxes matter?, *J. Geophys. Res.*, *104*, 13,235–13,249.

Wüst, G. (1935), Schichtung und Zirkulation des Atlantischen Ozeans: Das Bodenwasser und die Stratosphäre, in *Wissenschaftliche Ergebnisse der Deutschen Atlantischen Expedition auf dem Forchungs- und Vermessungsschiff 'Meteor' 1925–1927*, vol. 6, edited by W. Krauß and A. Defant, pp. 1–288, de Gruyter, Berlin.

R. P. Matano, College of Oceanic and Atmospheric Research, Oregon State University, 104 Ocean Admin Bldg., Corvallis, OR 97331, USA. (matano@coas.oregonstate.edu)

M. W. Schouten, Department of Physical Oceanography, Royal Netherlands Institute for Sea Research, Landsdiep 4, NL-1797 SZ Texel, Netherlands. (schout@nioz.nl)